

<Supplementary information>

**Self-assembled levan nanoparticles for targeted breast cancer imaging**

Sun-Jung Kim<sup>a</sup>, Pan Kee Bae<sup>b</sup>, Bong Hyun Chung<sup>abc\*</sup>

<sup>a</sup>BioNanotechnology Research Center, Korea Research Institute of Bioscience and Biotechnology (KRIBB), 125 Gwahak-ro, Yuseong-gu, Daejeon 305-806, Republic of Korea

<sup>b</sup>BioNano Health Guard Research Center, 125 Gwahak-ro, Yuseong-gu, Daejeon 305-806, Republic of Korea

<sup>c</sup>Nanobiotechnology Major, School of Engineering, University of Science and Technology (UST), 125 Gwahak-ro, Yuseong-gu, Daejeon 305-806, Republic of Korea

\*To whom correspondence should be addressed:

Bong Hyun Chung

Tel: +82-42-860-4442

Fax: +82-42-879-8594

E-mail: chungbh@kribb.re.kr

## **Materials and methods**

### 1. Materials

Levan (low (estimated MW<2000kDa) and high molecular weight (estimated MW>2000kDa)) was purchased from Realbiotech (Korea). Indocyanine green, 3-(4,5-dimethylthiazol-2-yl)-2,5-diphenyl tetrazolium bromide (MTT) and dimethyl sulfoxide (DMSO) were obtained from Sigma-Aldrich (Saint Louis, MO, USA). Roswell Park Memorial Institute medium 1640 (RPMI 1640) and Dulbecco's Modified Eagle Medium (DMEM) were purchased from Gibco BRL (Grand Island, NY, USA).

### 2. Formation of levan-ICG nanoparticles

Levan and indocyanine green nanoparticles were formed by self-assembly. Briefly, 0.5% of levan was dissolved in distilled water (10 ml) and 4 mg of indocyanine green was dissolved in water (1 mg/ml). The completely dissolved materials were mixed using a magnetic stirrer at 200 rpm for 24 h at room temperature. Unreacted ICG was removed by centrifugation at 13,500 rpm three times. The precipitate was redispersed in water and stored at 4 °C

### 3. Characterization of self-assembled nanoparticles

The morphology and size of the nanoparticles were characterized by transmission microscopy (TEM, CM20, Philips, The Netherlands) after loading the conjugate onto a carbon-coated copper grid and drying in air and dynamic light scattering (DLS, Otsuka Electronics, Osaka, Japan). The absorbance of the nanoparticles was measured by UV-Vis spectroscopy. To disassemble nanoparticles, Tween X-100 solution (0.1%) was incubated with nanoparticles.

#### 4. Efficiency of ICG encapsulation and release of ICG.

The efficiency of ICG encapsulation and release of ICG were confirmed by UV-Vis spectroscopy. 0.1 mg of levan-nanoparticles were dissolved in Tween X-100 solution and sonicated for 5 min to disassemble nanoparticle. The absorbance of disassembled nanoparticles was measured by UV-Vis spectroscopy at 780 nm. The amount of ICG in levan nanoparticles was estimated by comparing of ICG absorbance calibration curve. The percentage efficiency of ICG encapsulation was calculated by Eq. (1):

$$\text{ICG encapsulation efficiency (\%)} = \frac{\text{Mass of ICG in particles}}{\text{Mass of ICG used}} \times 100 \quad (1)$$

The release of ICG from nanoparticles was also measured by UV-Vis spectroscopy. One milligram mg of nanoparticles was dissolved in 1 ml of distilled water. The nanoparticle was dialyzed in phosphate buffer saline (PBS (pH 7.4)) solution using dialysis membrane (MWCO 14,000) for various times. The nanoparticles were centrifuged at 13,500 rpm. The supernatant was removed and then the precipitates were redispersed in distilled water. The release percentage of ICG from nanoparticles was estimated by adsorption spectra.

#### 5. Cellular cytotoxicity

The cellular cytotoxicity was evaluated using the MTT assay. MDAMB231 breast cancer cells ( $1 \times 10^4$  cells/well) were incubated in 96-well cell culture plates using RPMI 1640 medium containing 10% FBS and penicillin streptomycin for 24 h. Various concentrations of nanoparticles were then added to the medium and incubated with the cells for 24 h. After 24 h, the cells were washed with phosphate-buffered saline (PBS) and given fresh culture medium. Then, 10  $\mu$ l of MTT solution (5 mg/ml in PBS) was added for 4 h. The cells were washed, and

the formazan salt produced was dissolved in dimethyl sulfoxide (DMSO; 100  $\mu$ l). The absorption was measured at 570 nm using a microplate reader (SpectraMax M2, Molecular Devices).

## 6. Cellular uptake of nanoparticles

To observe cellular uptake of the nanoparticles, MDAMB231, A549, HeLa, SKOV3, KB and NIH3T3 cells were seeded in 8-well chamber slides ( $1 \times 10^4$  cells/well) for 24 h. The cells were then treated with levan-ICG nanoparticles for 1 h at 37 °C, washed with PBS three times, and then fixed with 4% paraformaldehyde for 10 min. The nuclei were stained using a solution of 4',6-diamidino-2-phenylindole (DAPI) for 5 min. Nanoparticle uptake by the cells was then observed by confocal microscopy (LSM 510 META, Zeiss, Oberkochen, Germany). The inhibition assay was performed using mercuric chloride (3 mM). MDAMB231 cells ( $1 \times 10^4$  cells/well) were incubated with levan-ICG nanoparticles, which were dissolved in medium containing mercuric chloride for 4 h. The cells were then washed, and the uptake of nanoparticles was observed by confocal microscopy. The inhibition assay also performed using fructose, levan and Glut5 antibody. Fructose, levan, and Glut5 antibody were preincubated with MDAMB231 cells for 1 h. After washing, the levan-ICG nanoparticles were incubated with cells for 1 h. The cells were then washed, and the uptake of nanoparticles was observed by confocal microscopy.

## 7. Interaction of levan and glucose transporter 5

To confirm the interaction of levan and glucose transporter 5, we used a modified ELISA method. A variety of concentrations of levan, fructose and BSA were incubated and in 96-well ELISA plates (Corning, Tewksbury, MA, USA) for 4 h at 37 °C. After washing, the plates were

incubated with 1% BSA to prevent nonspecific binding. Recombinant glucose transporter 5 (0.05 µg/ well, Abnova) was added to the plates for 2 h. After washing, biotin-conjugated glucose transporter 5 antibody (dilution 1:100, Cusabio, Wuhan, China) was added for 1 h. After washing, the horseradish peroxidase (HRP)-conjugated avidin (dilution 1:100, Cusabio, Wuhan, China) was incubated for 2 h at 37 °C. After washing, detection of GLUT5 binding was subsequently performed using TMB for 30 min, after which stop solution was added. The absorbance (450 nm) was measured on a microplate reader.

#### 8. Western blotting

Western blotting was performed to analyze proteins extracted from cells. Briefly, protein samples were obtained by lysing the cells using RIPA buffer (GeneDepot, Barker, TX, USA) and then centrifuging at 13000 rpm for 30 min at 4 °C. The protein concentration was quantified using the Bradford assay kit (GeneDepot). Protein separation was performed using 10% sodium dodecyl sulfate polyacrylamide gel electrophoresis (SDS PAGE), followed by transfer to a poly(vinylidene difluoride) (PVDF) membrane.

#### 9. Generation of tumor-bearing mice

Tumor-bearing mice were generated by subcutaneously injecting MDAMB231 cells ( $5 \times 10^6$  cells/200 µl PBS) into the right flanks of 5- to 6-week-old BALB/c nude mice (SLC, Inc., Hamamatsu, Japan). All animal care and experiments were approved by the Animal Care Committees of the Korea Research Institute of Bioscience and Biotechnology (KRIBB).

#### 10. *In vivo* and *ex vivo* imaging

The imaging and biodistribution of nanoparticles were observed using an IVIS imaging system after the nanoparticles were injected intravenously. Briefly, 200  $\mu$ l of a nanoparticle stock solution (10 mg/ml) was injected into the tail veins of the mice. The mice were then observed on an IVIS Lumina imaging system (Xenogen, Alameda, CA, USA) using an ICG filter set 1 and 2 days after the injection. To observe the biodistribution of the nanoparticles, the mice were sacrificed 2 days after injection of the nanoparticles, and their livers, spleens and kidneys were observed on the imaging system.

#### 11. Histochemical analysis

The tumor tissue was fixed with formalin and cryosectioned. The sections were blocked with a 1% BSA solution and permeabilized with 0.1% Triton X-100 for 2 min at room temperature. The nuclei were stained using a DAPI solution. The samples were then observed by confocal microscopy.

#### 12. Statistical analysis

The experiments were independently performed in triplicate, and the results are expressed as the mean  $\pm$  standard deviation. Statistical significance was determined by Student's t-test. A probability (*p*) value of  $<0.05$  was considered statistically significant.

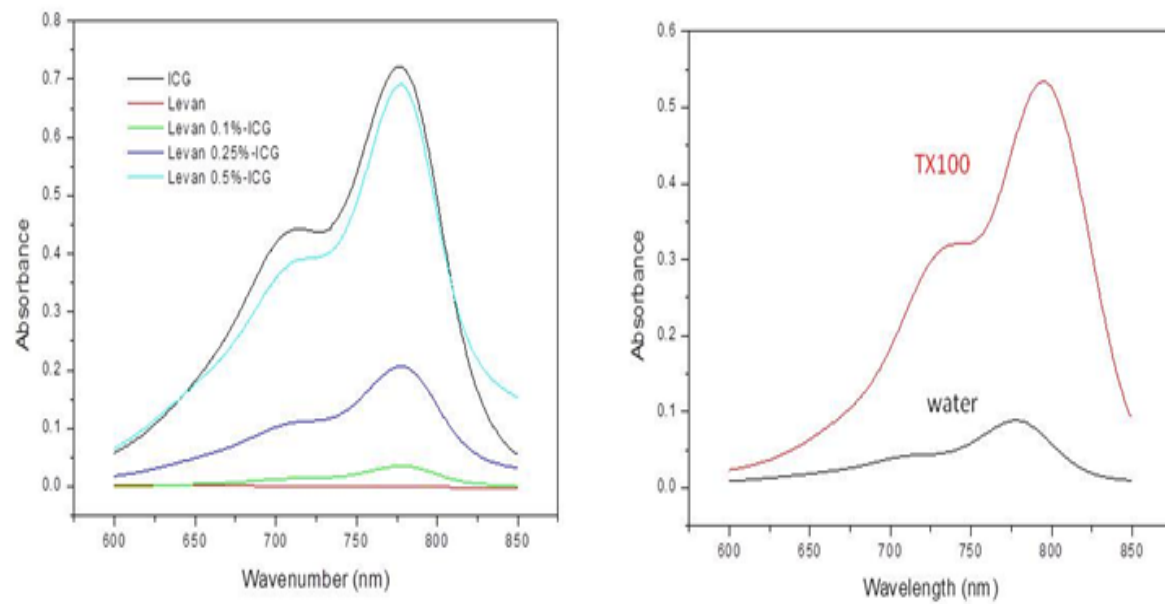
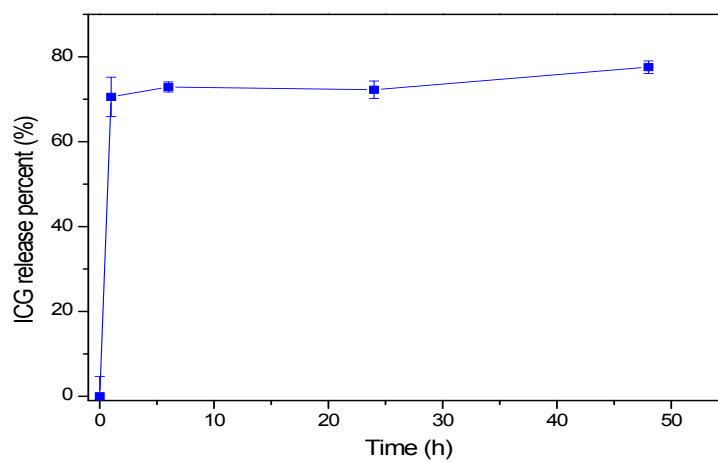


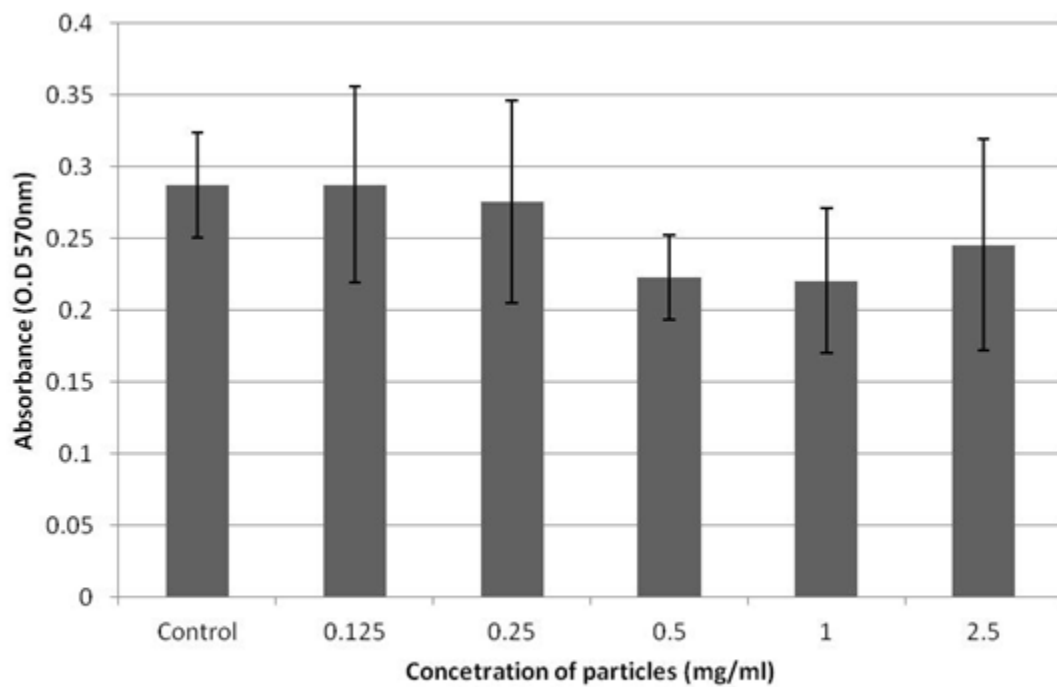
Fig S1. A) Absorbance of levan-ICG nanoparticles (ICG conjugated with different concentrations of levan). (B) Absorbance of levan-ICG nanoparticles in water and 0.1%TX-100 obtained by UV-Vis spectroscopy

Molecular weight of levan	Mixing speed	Size of particles	Efficiency of ICG encapsulation
Low	200rpm	138.5±34.1nm	14.275%
Low	1000rpm	229.2±41.5nm	28.4%
High	200rpm	202.1±46.8nm	12.65%

Table S1. Characterization of levan-ICG nanoparticles

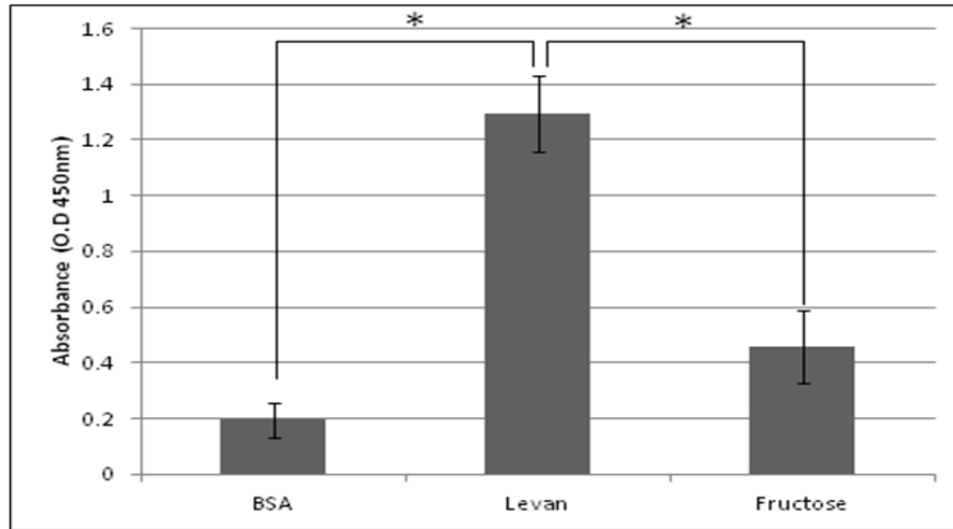


FigS2. The release profile of ICG from levan-ICG nanoparticles (n=3)



FigS3. Cytotoxicity of assembled nanoparticles to MDAMB231 cells. Cell viability was calculated from the MTT assay. The data are shown as the mean  $\pm$  SD (n = 3).

(A)



(B)

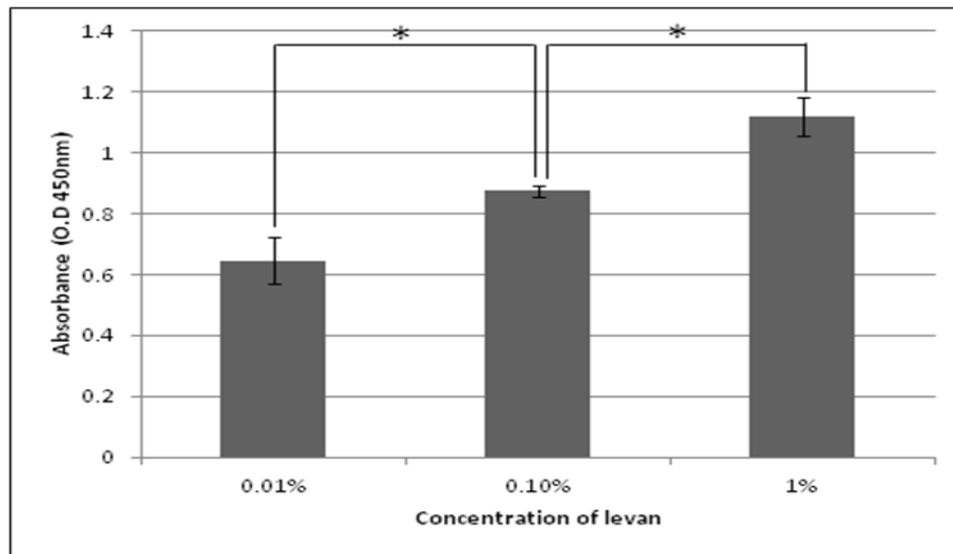
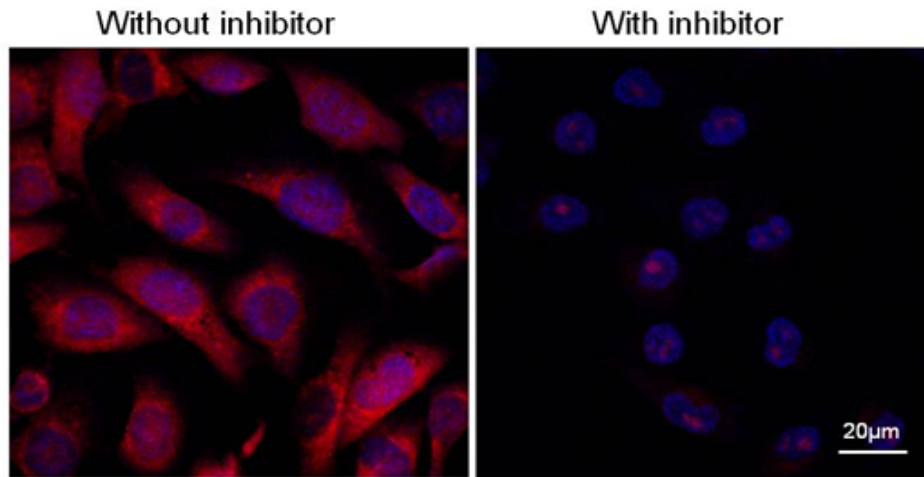
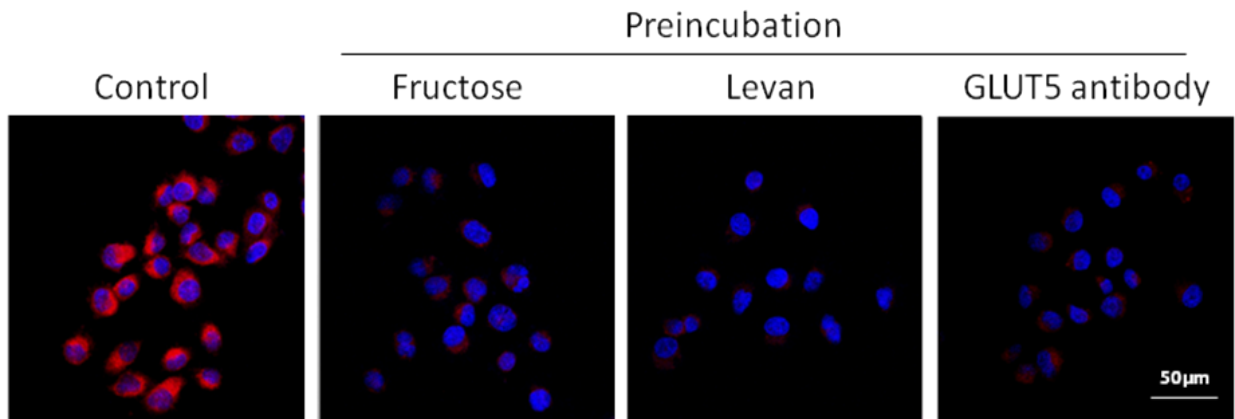


Fig S4. (A) Interaction of levam and glucose transporter 5, measured by a modified ELISA assay. (B) Interaction of glucose transporter 5 according to concentration of levam .The data are shown as the mean  $\pm$  SD (n = 3, p<0.05)

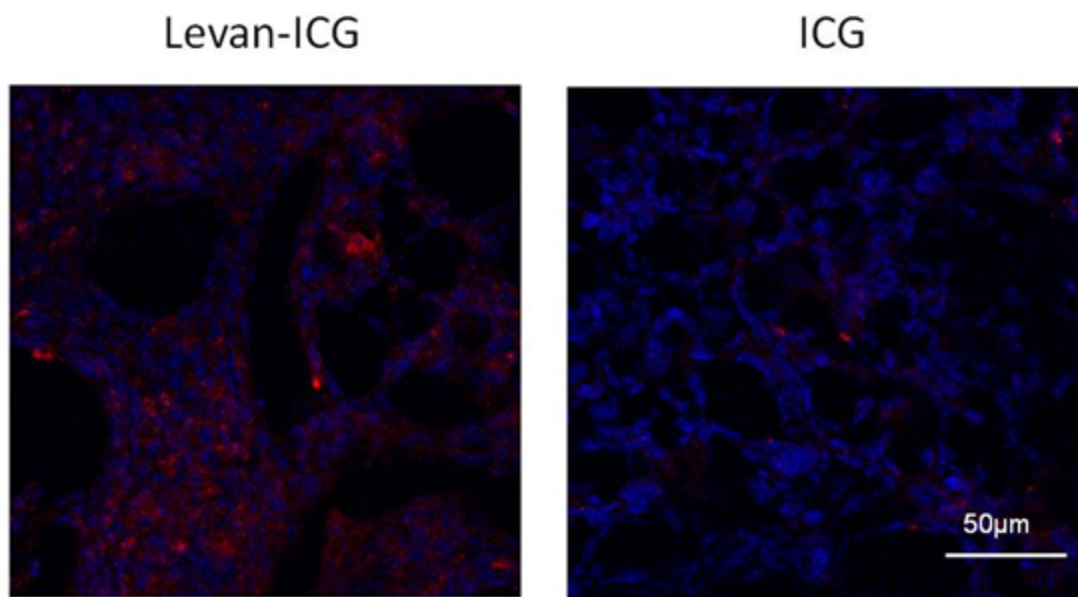
(A)



(B)



FigS5. (A) Cellular uptake of ICG-encapsulating levan nanoparticles with and without inhibitor (B) Cellular uptake of ICG-encapsulating levan nanoparticles after preincubation of fructose, levan and Glut5 antibody. (Red: ICG-encapsulating levan nanoparticles, Blue: DAPI).



FigS6. Histochemical analysis of tumor cryosections by confocal microscopy after injection of levan-ICG nanoparticles (left) and ICG only (right; Red: ICG, Blue: DAPI).